Vulnerable Carotid Atherosclerotic Plaque Creation in a Swine Model: Evaluation of Stenosis Creation Using Absorbable and Permanent Suture in a Diabetic Dyslipidemic Model

Gilles Soulez, MD, MSc, Sophie Lerouge, PhD, Louise Allard, PhD, Philippe Roméo, MD, Shijie Qi, MD, Hélène Héon VMD, Jean-Claude Tardif, MD, and Guy Cloutier, PhD

ABSTRACT

Purpose: To compare the creation of carotid atherosclerotic plaque after stenosis creation with absorbable or permanent suture in a diabetic dyslipidemic swine model.

Materials and Methods: A high-cholesterol diet was fed to 15 Sinclair pigs. Diabetes was induced by intraarterial injection of streptozotocin. Stenosis creation in carotid arteries was performed with an absorbable or a permanent suture assigned randomly on both sides. After 20 weeks, Doppler ultrasound (US), angiography, and intravascular US examinations were performed before sacrifice. Carotid, coronary, and femoral arteries were analyzed by histology according to the American Heart Association (AHA) classification.

Results: Three animals died during the perioperative period, and three others died during follow-up. Diabetes was successfully induced in all surviving animals (9 of 15). On angiography, stenoses were estimated at 80.4%±12.4 in carotid arteries with permanent sutures and at 48.8%±39 with absorbable sutures ($P = .03$). With permanent suturing, carotid plaques were observed in all animals with five of nine manifesting an AHA stage IV or more. With absorbable suture, atherosclerosis developed in seven of nine carotid arteries including three animals with an AHA stage IV or more. Advanced coronary and femoral plaques were observed in four and one of the nine animals. A correlation between AHA classes of coronary plaques and cholesterol level was observed ($P = .01$), whereas for carotid arteries, AHA class correlated with the degree of stenosis ($P = .045$).

Conclusions: Creation of atheromatous lesions in carotid and coronary arteries was successful with this model despite a high mortality rate. Less severe carotid stenoses and advanced plaques were observed with absorbable sutures.

ABBREVIATIONS

AHA = American Heart Association, GTT = glucose tolerance test

From the Department of Radiology (G.S.), University of Montreal Hospital Center (CHUM), Hôpital Notre-Dame, 1560 Sherbrooke Street East, Montréal, Québec, Canada H2L 4M1; Department of Radiology, Radio-Oncology and Nuclear Medicine (G.S., S.L., G.C.), Institute of Biomedical Engineering (G.S., S.L., G.C.), Department of Pathology (P.R.), University of Montreal; Laboratory of Endovascular Biomaterials (S.L.), Laboratory of Biorheology and Medical Ultrasonics (L.A., G.C.), Core Imaging Laboratory (G.S.), Experimental Surgery (S.Q.), Animal Laboratory (H.H), University of Montreal Hospital Research Center (CRCHUM), Department of Mechanical Engineering (S.L.), Ecole de technologie supérieure; and Department of Cardiology (J.-C.-T.), Montreal Heart Institute, Montréal, Québec, Canada. Received April 1, 2012; final revision received August 28, 2012; accepted September 3, 2012. **Address correspondence to** G.S.; E-mail: gilles.soulez.chum@ssss.gouv.qc.ca

This work was supported by a clinical research scholarship (to G.S.) from the Fonds de la Recherche en Santé du Québec (FRSQ) and operating grants from the Natural Sciences and Engineering Research Council of Canada and the Canadian Institutes of Health Research (NSERC—Collaborative Health Research Projects Program, grants NSERC 323405-06 and CIHR CPG-80085).

Figures E1–E8 and Table E1 are available online at *www.jvir.org*.

None of the authors have identified a conflict of interest.

The authors are grateful to Elisabeth Mercure for her assistance during ultrasound examination and all the staff of CRCHUM animal laboratory for the excellent care given to animals during this study.

© SIR, 2012

J Vasc Interv Radiol 2012; 23:1700–1708

http://dx.doi.org/10.1016/j.jvir.2012.09.001

About 60% of ischemic strokes in Western countries are caused by the rupture of a vulnerable atherosclerotic carotid plaque (1,2). Various mouse models of plaque development have been created in deficient apolipoprotein E or low-attenuation lipoprotein-receptor knockout mice (3). A large animal model of vulnerable carotid plaque is necessary to elucidate the disease natural history and to test imaging biomarkers and new therapeutic interventions applicable to human patients. Swine have proven to be an excellent model for cardiovascular studies. The cardiovascular system in swine is nearly identical to the cardiovascular system in humans, and they spontaneously develop coronary artery disease, which is accelerated by a high-fat, high-cholesterol diet and diabetes (4). A combination of diabetes induction with intravenous injection of alloxan or streptozotocin and high-fat diet in a miniature pig model mimicked vascular complications observed in human diabetic dyslipidemia (5–7). With this model, according to the American Heart Association (AHA) classification (8,9), advanced and complex atherosclerotic plaques were observed after 12–36 weeks in coronary arteries, iliac arteries, and aorta, and much less significant lesions were observed in carotid arteries (5,10).

The balloon injury approach has been used to simulate atherosclerosis-like lesions (11). When combined with hypercholesterolemia, these lesions do not reproduce vulnerable atherosclerotic plaques in carotid arteries (12,13). The balloon injury model is also limited by a significant incidence of thrombotic occlusion (14). More recently, a model combining the creation of carotid stenosis with a suture and a dietary hypercholesterolemia has been reported (15,16). This approach induces more advanced carotid atherosclerotic lesions with fewer thrombotic occlusions (15,16). There is no documentation of atherosclerotic disease outside the carotid artery bed with this model. One limitation of stenosis creation with a permanent suture is the artificial narrowing of the vessel impairing imaging studies or interventional procedures. In this study, we combined diabetic induction with dietary hypercholesterolemia in minipigs to accelerate atherosclerotic formation in coronary, femoral, and carotid arteries by stenosis creation with permanent or absorbable suture to compare the efficacy of both approaches.

MATERIALS AND METHODS

Protocols for animal experiments were approved by the animal care committee of our research center, in accordance with the guidelines on the care and use of laboratory animals issued by the Canadian Council on Animal Care and the U.S. National Institutes of Health (assurance number A5377-01). We enrolled 15 Sinclair male minipigs (Sinclair Research Center, Auxvasse, Missouri) with a mean age of 211 days ± 36 and weight of 35 kg ± 8 in the study.

Carotid Ligation

Using the surgical technique reported by Ishii et al (15), common carotid arteries were partially ligated with a 1.3-mm spacer on the external surface of the vessel, 4 cm below the internal-external carotid bifurcation. This spacer was subsequently removed before closing the incision, leaving a 70%–80% stenosis. On one side, a permanent suture was positioned (4-0 Prolene 8204, Ethicon blue monofilament polypropylene; Ethicon, Cornelia, Georgia) as originally described by Ishii et al (15), whereas the other side was ligated with an absorbable suture (4-0 Vicryl J504, Ethicon braided polyglactin 910; Ethicon). The type and side of suture were randomly allocated.

Diabetes Induction

Diabetes was induced 1 week after surgery by selective injection of streptozotocin (120 mg/kg) injected via a 4-F Glidecath catheter (Terumo, Tokyo, Japan) inserted through a femoral approach. The dose was divided and injected selectively, 60% in the proximal portion of the splenic artery and 40% in the proximal gastroduodenal artery as reported by Tal et al (17) in a primate model. Blood glucose was closely monitored during the first 48 hours because of the risk of hypoglycemia secondary to acute lysis of pancreatic beta cells. To facilitate blood sampling and intravenous medication administration, a 9-F single-lumen central catheter ($n = 5$) (Hickman; Bard Medical, Salt Lake City, Utah) or implantable port ($n = 4$) (Bard Medical) was placed through the right or left internal jugular vein and tunneled in the posterior portion of the neck. After 1 week, if serum glucose was < 10 mmol/L, a second streptozotocin injection using the same protocol was repeated (3 of 15 pigs).

High-fat Diet

All animals were fed a high-fat, high-cholesterol diet (TD.96366 Swine High-fat Diet; Harlan Teklad, Madison, Wisconsin) to induce hypercholesterolemia. The diet was started 7 days after diabetes induction and continued for the 20-week duration of the study until the time of sacrifice. Growth in weight was maintained at approximately 1% body weight gain per week.

Medication

All animals received a low dose of aspirin (80 mg) 10 days before and 30 days after surgery. In the first three animals, aspirin was continued for the duration of the study. During the perioperative period, 9 of the 15 enrolled animals received enoxaparin injection for 1–10 days to prevent carotid thrombosis when a slow flow in the carotid artery was observed distal to the stenosis. One pig needed insulin therapy during the last month of follow-up because of the appearance of type 1 diabetes. Other medications were given during the perioperative period to control postoperative pain (fentanyl, morphine, meloxicam, bupivacaine) or infection (enrofloxacin).

Biologic Profile

Every month, blood samples were taken for assay of glucose, serum creatinine, total cholesterol, high-density lipoprotein cholesterol, and low-density lipoprotein cholesterol. A glucose tolerance test (GTT) was performed after injection of 50 g of glucose intravenously 3 months after diabetes induction.

Imaging Protocols

External Ultrasound Examination of Carotid Arteries. All ultrasound (US) examinations were performed under general anesthesia. Permanent tattoos were marked on the skin at the level of the carotid bifurcation and each 1 cm upstream for a distance of 8 cm to guide follow-up examinations. US studies (Ultrasonix, Vancouver, BC, Canada) were performed at baseline and at 4, 8, 12, 16, and 20 weeks (date of sacrifice) after diabetes induction. B-mode measurements of luminal diameters were taken on axial and longitudinal views for each tattooed segment followed by color Doppler and duplex evaluations. The percent stenosis was calculated by measuring the ratio between the minimal diameter in the stenosis and the diameter in a reference segment proximal or distal to the stenosis. For stenoses of $>$ 50%, the severity of the lesion was graded according to the maximal systolic velocity and its ratio with the velocity taken proximal to the stenosis, according to recognized criteria (18). Near occlusion with diffuse narrowing of the artery secondary to severe stenosis or partial thrombosis was classified as a 95% stenosis. Color duplex studies were also performed on both common femoral arteries at the same time as the carotid artery studies.

Carotid Artery Angiography and Intravascular US. Before sacrifice at 20 weeks, selective catheter angiography of both carotid arteries was performed through a femoral approach with a 4-F Glidecath catheter (Terumo). Diameter of stenoses was measured, and the reference diameter was taken in a normal segment of the common carotid artery. In the presence of near occlusion, the stenosis was graded at 95% as proposed in the North American Symptomatic Carotid Endarterectomy Trial criteria (19).

An intravascular US study was done on both carotid arteries using an automatic pullback system set at 0.5 mm/s with a 3.5-F 20-MHz array probe (AVANAR F/X, 20 MHz; Volcano Therapeutics, Rancho Cordova, California). Minimal lumen areas were measured in the stenosed segment and compared with the mean luminal surface of reference segments to calculate the maximal luminal stenosis in area percentage. In the presence of near occlusion, the surface stenosis was also graded at 95%. The plaque area was calculated as the difference between the manually segmented vessel area and lumen area at the level showing the largest plaque burden. Plaque echogenicity was classified on a four-grading scale (1, hyperechoic; 2, isoechoic; 3, hypoechoic; and 4, heterogeneous), and the presence of calcification was noted.

Coronary Artery Angiography and Intravascular US. All pigs underwent angiography of the left and right coronary arteries followed by a 40-MHz automated intravascular US pullback set at 0.5 mm/s (Galaxy II; Boston Scientific, Nattick, Massachusetts) of the three principal arterial branches (right, left main with interventricular anterior, and left circumflex) whenever possible. The same protocol described previously for carotid arteries was followed for stenosis quantification and characterization with angiography and intravascular US. Animals were sacrificed at the end of the procedure.

Histologic Sections

Carotid and coronary arteries were perfused with saline for 5 minutes followed by 10% buffered formalin at 150 mm Hg for 1 hour. After localization of the carotid bifurcation and carotid segments corresponding to external tattoos, left and right carotid arteries were harvested with coronary arteries and fixed in buffered formalin before paraffin embedding. Femoral arteries were also harvested in seven of the nine animals. We performed 6-μm-thick sections every 5 mm and added serial sections when a plaque was detected. Three stains were employed. Hematoxylin phloxine saffron stain was used to differentiate collagen (yellow), nuclei (blue), and muscle and cytoplasm (pink). The Movat stain was chosen to differentiate elastic fibers (black), collagen (yellow-green), nuclei (dark blue), cytoplasm (pink-brown), and calcium (brown). If Movat staining suggested the presence of calcium, a more quantitative von Kossa stain was employed to highlight calcium nodules in black. Picrus-sirius red stain was also used for collagen analysis and for grading intimal thickening in AHA stage I–III lesions.

Plaques were classified according to the AHA classification that summarizes the natural history of atherosclerosis (**Table 1**) (8) by a pathologist blinded to the location or type of suture. Histomorphometric analyses were performed with Image J software (NIH open source,

Table 1. Modified American Heart Association Classification of Atherosclerotic Lesions

Lesion Type	Description
I	Initial lesion with foam cells (intimal xanthoma or fatty streak)
II	Fatty streak with multiple foam cell layers
III	Preatheroma with extracellular lipid pools
IV	Atheroma with a confluent extracellular lipid core
V	Fibroatheroma
VI	Complex plaque with possible surface defect or hemorrhage or thrombus or some combination
VII	Calcified plaque
VIII	Fibrotic plaque without lipid core

Adapted from Stary HC. Natural history and histological classification of atherosclerotic lesions: an update. Arterioscler Thromb Vasc Biol 2000; 20:1177–1178.

Bethesda, Maryland) and with in-house semiautomatic segmentation software developed on Matlab (version 6.5; MathWorks Inc., Natick, Massachusetts). Minimal lumen, plaque area, and plaque localization in regard to the carotid bifurcation were determined for each plaque. Plaque area was calculated as vessel area minus lumen area. Vessel area was defined as the area within the media or adventitial border.

Data Analysis

The carotid bifurcation or the origin of coronary vessel served as a reference to match angiography, Doppler US, intravascular US cross-sectional, and histologic cross-sectional images. On intravascular US, knowing the pull-back speed and the frame rate permitted calculation of the distance between the bifurcation and the plane of view. For carotid arteries, the degree of maximum stenosis was determined on digital subtraction angiography and intravascular US and used as a positioning reference in addition to the vessel bifurcation.

For histologic sections, the distance was measured with a caliper between the bifurcation and the section to cut. The slices corresponding to the area of maximal stenosis and the position of the suture and of the more advanced plaque were noted with their respective distance from the carotid bifurcation. A descriptive analysis of the plaque distribution, position, and grading according to the type of suture was performed. The distribution and characteristics of the more advanced (AHA criteria) coronary and femoral plaques were also analyzed.

Mean cholesterol and glucose levels between 4 and 20 weeks were calculated. The Pearson correlation between these data and AHA classification in carotid and coronary arteries were performed using SPSS (version 17; SPSS, Inc, Chicago, Illinois). The same analysis was done to correlate plaque classification according to AHA criteria and the degree of stenosis on Doppler US at 20 weeks. For these analyses, stage V–VIII plaques were classified as V or more. Mean percentage of stenosis on angiography and plaque volume on histology were compared between the groups with absorbable and permanent sutures with a Student *t*-test. The level of significance was set at 0.05.

RESULTS

Mortality

During the perioperative period, 3 of the 15 animals (20%) died. One animal had a cardiac arrest during surgery because of verapamil overdose. A second had a stroke 2 days after surgery. The last one injured itself in its cage 22 days after surgery and was euthanized. Three other animals died during follow-up (20%). One died 72 days after surgery because of streptozotocin-induced renal failure. A second died 64 days after surgery of ventricular fibrillation during the replacement of a central venous catheter. Another had a cardiac arrest 100 days after surgery during a prolonged anesthesia for Doppler US examination. The results of nine animals (60%) that completed the study with 20-week follow-up are reported.

Change in Glucose Measurement

The evolution of fasting glucose level for the nine pigs is detailed in **Figure E1** (available online at *www.jvir.org*). The mean values were estimated at 3.3 mmol/L ± 1.2 at baseline and 15.4 mmol/L ± 4.0, 12.7 mmol/L ± 5.2, 11.6 mmol/L ± 3.9, 13.0 mmol/L ± 5.1, and 13.0 mmol/L ± 5.4 at 4 weeks, 8 weeks, 12 weeks, 16 weeks, and 20 weeks. Seven pigs were clearly diabetic throughout the duration of the study. One pig (no. 3) (pig numbers refer to **Tables 2, 3,** and **E** [**Table E1** is available online at *www.jvir.org*]) was diabetic at week 4 but returned to normal fasting glucose between 8 and 20 weeks and had a normal glucose value (5.3 mmol/L) 2 hours after a GTT. Another pig (no. 5) had fasting glucose values estimated at 6.9 mmol/L, 4.5 mmol/L, 4.5 mmol/L, 4.3 mmol/L, and 6.3 mmol/L at 4 weeks, 8 weeks, 12 weeks, 16 weeks, and 20 weeks with a 15.7 mmol/L value 2 hours after a GTT. According to the American Diabetes Association (range for humans with fasting glucose intolerance of 5.6–6.9 mmol/L and values after GTT of 7.8–11.0 mmol/L) and recognized glycemia values for Sinclair pigs (fasting glucose value of 3 mmol/L and 17 mmol/L in control pigs and diabetic pigs with high-fat diet), this last animal had a borderline status between glucose intolerance and diabetes (20,21).

The weight curves during the study are shown in **Figure E2** (available online at *www.jvir.org*). The mean weight gain was estimated at 39% ± 112. Only two animals lost weight during follow-up (−31% and −8%). The latter developed type 1 diabetes with ketoacidosis and required insulin therapy.

Lipid Profile

The evolution of the lipid profile is shown in **Figure E3** (available online at *www.jvir.org*). The mean values of total cholesterol levels were estimated at 2.5 mmol/L ± 0.4, 14.4 mmol/L ± 9.1, 25.7 mmol/L ± 21.7, 28.9 mmol/L ± 22.4, 32.4 mmol/L ± 26.6, and 21.0 mmol/L ± 16.9 at baseline, 4 weeks, 8 weeks, 12 weeks, 16 weeks, and 20 weeks. Low-density lipoprotein cholesterol levels were estimated at 1.0 mmol/L ± 0.4, 9.9 mmol/L ± 5.8, 14.2 mmol/L ± 9.5, 15.4 mmol/L ± 10.8, 15.9 mmol/L ± 11.3, and 10.7 mmol/L ± 7.0.

Carotid Stenosis Evolution

The evolution of carotid stenoses on Doppler US for permanent and absorbable sutures is shown in **Figure E4a** and **b** (available online at *www.jvir.org*). In the group with stenosis with permanent suture, the degree of stenosis ranged from 59%–95% with three near occlusions noticed at 1 month, 2 months, and 4 months. Besides these three near occlusions, severity of stenosis was quite stable during the study period.

In the group with absorbable sutures, the degree of stenosis ranged from 11%–95%. Three near occlusions

Table 2. Digital Subtraction Angiography, Intravascular Ultrasound, and Histomorphometric Characteristics of Carotid Stenoses and Plaque after Creation of Stenosis with Permanent Suture

	Permanent Suture						
Pig No.	% Stenosis Diameter DSA	% Stenosis Area Intravascular US	Ligation Distance, mm	Plaque Distance	Plaque Intravascular US	Plaque Area Histology, mm^2	Plaque AHA Grade
1	73	64	46	0	hyper	0.70	II/III Ca
2	71	68	68	66	hetero	0.46	IV
3	86	75	38	75	hetero	1.47	VIII
4	70	65	34	30	hypo	0.81	VI Ca
5	95	95	33	28	hyper	0.27	III
6	75	80	32	35	iso	0.15	II Ca
7	95	NA*	40	18	NA*	1.27	VII Ca
8	64	64	28	34	hypo	0.43	II
9	95	95	27	40	hypo	1.22	V

% Stenosis Diameter DSA = measurement of the degree of stenosis in diameter on angiography, % Stenosis Area Intravascular US = measurement of the degree of stenosis in area on intravascular US, Plaque Distance = distance between the carotid bifurcation and the most advanced plaque, Plaque Intravascular US = evaluation of plaque echogenicity on intravascular US (hetero = heterogeneous; hyper = hyperechogenic, hypo = hypoechogenic, iso = isoechogenic), Plaque Area Histology = plaque area measurement in mm^2 on histology, Plaque AHA Grade = plaque evolution according to the AHA classification, AHA = American Heart Association, Ca = calcification, DSA = digital subtraction angiography, US = ultrasound, *NA = not available (in pig no. 7, owing to the near occlusion, it was not possible to advance the intravascular US probe in the ligated segment).

Table 3. Digital Subtraction Angiography, Intravascular US, and Histomorphometric Characteristics of Carotid Stenoses and Plaque after Creation of Stenosis with Absorbable Suture

	Absorbable Suture						
Pig No.	% Stenosis Diameter DSA	% Stenosis Area Intravascular US	Ligation Distance, mm	Plaque Distance	Plaque Intravascular US	Plaque Area Histology, mm^2	Plaque AHA Grade
1	0	9	20	0	hyper	0.06	II Ca
2	40	51	45	45	hetero	0.61	IV
3	95	95	34	—	—	—	I
4	26	49	43	(63)	hypo	(2.6)	III
5	95	95	40	—	—	—	I
6	0	15	25	(31)	hypo	(2.4)	III
7	58	76	22	70	hypo	0.08	IV
8	30	31	24	22	hetero	6.94	V Ca
9	95	95	27	36	iso	1.6	V Ca

% Stenosis Diameter DSA = measurement of the degree of stenosis in diameter on angiography (95% stenosis was calculated in case of near occlusion), % Stenosis Area Intravascular US = measurement of the degree of stenosis in area on intravascular US (95% stenosis was calculated in case of near occlusion), Plaque Distance = distance between the carotid bifurcation and the most advanced plaque (values in parentheses are taken from intravascular US acquisitions), Plaque Intravascular US = evaluation of plaque echogenicity on intravascular US (hetero = heterogeneous, hyper = hyperechogenic, hypo = hypoechogenic, iso = isoechogenic), Plaque Area Histology = plaque area measurement in mm^2 on histology (values in parentheses are taken from intravascular US acquisitions), Plaque AHA Grade = plaque evolution according to the AHA classification, AHA = American Heart Association, Ca = calcification, DSA = digital subtraction angiography, US = ultrasound.

were noticed, two at 1 month and one at 3 months. In two of these three animals, bilateral near occlusions were observed (permanent and absorbable sutures). In the six remaining cases, a decrease of severity of stenosis was observed throughout the study period.

The degrees of maximal stenosis before sacrifice on angiography (diameter) and intravascular US (area) are listed in **Tables 2** and **3**. The mean degree of maximal stenosis on digital subtraction angiography was significantly higher in the group with permanent sutures (80.4% ± 12.4) compared with the group with absorbable sutures (48.8% ± 39.0; $P = .03$). In the absorbable suture group, no residual stenosis was observed in two carotid arteries.

Characteristics of Carotid Plaque Formation According to Suture Type

For permanent sutures, all arteries manifested at least a stage II atherosclerotic plaque with five of nine manifesting potentially vulnerable stage IV–VIII lesions (**Table 2** and **Figs 1** and **E5a–d** [available online at *www.jvir.org*]). Two of these advanced lesions were observed in carotid arteries having a near occlusion (**Figs 2a** and **b** and **E6a** and **b** [available online at *www.jvir.org*]). Plaques were located in the vicinity (within 10 mm) of the ligation in five cases, cranial to the suture in two cases, and caudal to the suture in two cases.

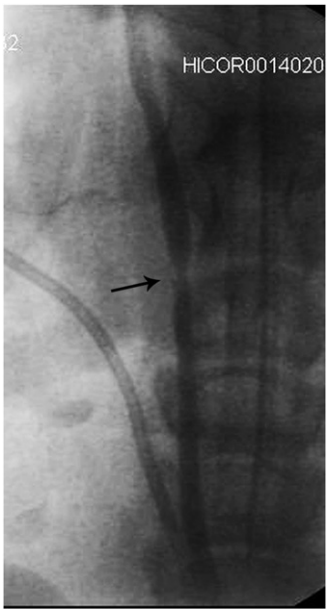

Figure 1. Vulnerable carotid plaque localized in the vicinity of a permanent suture (pig no. 4). Selective angiography of the right carotid artery shows 70% stenosis related to the permanent suture with plaque formation (arrow).

In the group with ligation with an absorbable suture, seven of nine carotid arteries developed atherosclerosis including four with stage IV–V plaques (**Figs 3** and **E7a–c** [available online at *www.jvir.org*]) and three with stage II–III lesions (**Table 3**). Three lesions were in the vicinity of the suture, two were caudal to the suture site, and two were cranial to the suture site. One of the three carotids with a near occlusion developed a stage V atherosclerotic plaque (**Fig E6a** and **b** [available online at *www.jvir.org*]). The two pigs without atherosclerotic plaque displayed intimal thickening (stage I) in the area of the arterial suture.

The mean plaque area was estimated at 1.50 $mm^2 \pm 2.27$ in carotids with stenosis with absorbable sutures and 0.75 $mm^2 \pm 0.47$ for arteries with stenosis with permanent sutures ($P = .15$). Plaque area measurements were more variable in the absorbable suture group as shown by the standard deviation.

Characteristics of Coronary and Femoral Plaque Formation

Four pigs developed advanced (stage IV–VI) lesions in coronary arteries (**Fig E8a–c** [available online at *www.jvir.*

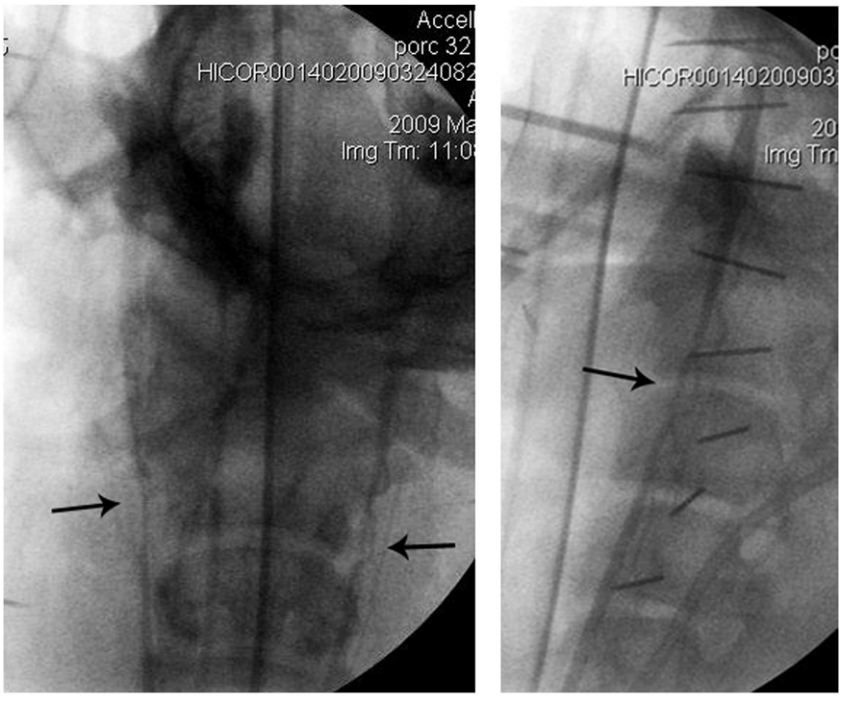

a. b.

Figure 2. Development of bilateral near occlusion with advanced plaque formation (pig no. 9). **(a)** Aortic arch angiography demonstrates a right carotid artery stenosis created with absorbable suture and a left carotid artery stenosed with a permanent suture. Both show near occlusions (95% stenosis by convention) with diffuse narrowing. High-grade stenoses are observed at both ligation areas (arrows). **(b)** Oblique and magnified projection on the left carotid artery shows diffuse narrowing (arrow).

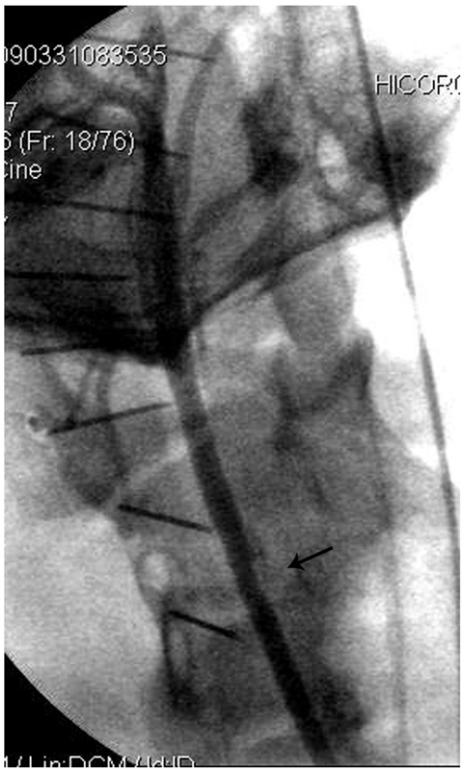

Figure 3. Development of an advanced atherosclerotic lesion after carotid artery stenosis creation with an absorbable suture (pig no. 8). Selective angiography of the right carotid artery shows a 30% stenosis in the vicinity of the suture site (arrow).

org]), whereas four had moderate type I and II lesions, and one had normal coronary arteries. Regarding femoral arteries, only one pig manifested advanced stage V atherosclerotic lesions (**Fig E8a–c** [available online at *www.jvir.org*]), whereas three had early type I or II lesions, and two had no lesion. Two pigs had no histologic analysis of femoral arteries for technical reasons. **Table E1** (available online at *www.jvir.org*) shows the distribution of coronary and femoral artery lesions according to the AHA classification.

Correlation between Carotid Plaque Formation, Glucose, Cholesterol Levels, and Carotid Stenosis Severity

A strong correlation was found between cholesterol levels between 4 and 20 weeks and AHA classification for coronary artery lesions ($R = 0.87$, $P = .001$) but not for carotid artery lesions ($R = 0.15$, $P = .56$). No correlation could be found between blood glucose and AHA classification for coronary ($R = 0.17$, $P = .38$) or carotid lesions ($R = 0.28$, $P = .27$). Finally, there was a correlation between the degree of stenosis on Doppler US at 20 weeks and AHA classification of carotid arteries ($R = 0.51$, $P = .045$).

DISCUSSION

In our model, we have combined hypercholesterolemia, diabetes mellitus, and creation of carotid stenosis to generate over a short period of time advanced atherosclerotic lesions (vulnerable plaques) in carotid and coronary arteries. Similar lesions were noted in the common femoral arteries of some animals. We have reproduced in pigs the pattern of atherosclerotic disease often associated with human metabolic syndrome (22,23).

Gerrity et al (6) reported advanced coronary, iliac, and aortic lesions in a model combining hypercholesterolemia and diabetes induction (with streptozotocin) in Yorkshire pigs within 20 weeks. However, the combination of diabetes induction and hypercholesterolemia did not create advanced carotid plaques. The same findings were reported by Dixon et al (5) in a hypercholesterolemia and alloxan-induced diabetes pig model and by Mohler et al (10) in a streptozotocin-induced diabetes model. In our study, there was a correlation between cholesterol level and plaque formation only in coronary arteries, whereas plaque characteristics were associated with the degree of stenosis in carotid arteries.

The concept of partial carotid ligature to create carotid plaques was proposed by Ishii et al (15) in hypercholesterolemic minipigs. The turbulent flow and low shear stress created by the stenosis stimulate plaque formation (24). These investigators compared partial ligation using permanent suture and balloon injury with a control group. They observed advanced stage IV and V plaques in 66% of carotid arteries with partial ligations and none in the balloon injury and control groups. Thrombotic occlusions were present in 33% of animals with balloon injury. In a second cohort of pigs, the same group reported advanced plaque in only 47% of carotid arteries (16). There was an association between the presence of advanced plaques and the occurrence of microembolism (70% vs 21%; $P < 0.02$) (16). In our study, similar results for plaque formation and classification were obtained with permanent sutures. However, we observed more near occlusions. This observation can be explained by more severe endothelial dysfunction secondary to induction of diabetes in our model.

Use of absorbable suture was associated with greater variability in plaque size and AHA histologic characteristics. Overall, more advanced atherosclerotic lesions were observed compared with previous series of hypercholesterolemic and diabetic pig models without creation of a carotid stenosis (5,6,10). Suturing with an absorbable suture created an initial severe stenosis followed by a stenosis regression over time. This approach is appealing because after several weeks, when the suture dissolved, only the plaque remained without artificial stenosis that could interfere with vessel hemodynamics and wall compliance. Plaques created using absorbable suture could represent a more clinically relevant model for the study of vessel wall or plaque mechanical characteristics (25) and

for testing interventional devices. However, suture dissolution can lead to inflammation and fibrosis in the vessel wall. This possibility should be kept in mind when validating molecular probes (26).

Miniature pigs are preferred for long-term studies because their limited growth facilitates handling and imaging (26). Yucatan, Hanford, Sinclair, Pitman-Moore and Hormel minipigs have been successfully used in atherosclerosis models (13,27). Diabetic hypercholesterolemic pigs gain weight at a slower rate than hyperlipidemic-only pigs (26); this was confirmed by a 38% mean growth over 5 months in our study.

We observed a high mortality rate despite careful animal care (40%); this is explained by the complexity of the model requiring diabetes induction and carotid surgery, exposing the animal to a combined surgical and metabolic stress. Because these animals underwent multimodal experimental imaging techniques, they were exposed to repeated and prolonged anesthesia. Three of the animals died during anesthesia for surgical or imaging manipulations. Two died because of specific complications of the model (stroke secondary to the surgical ligature and renal failure secondary to repeated streptozotocin injection). There is also a learning curve effect because four of the six deaths occurred in the first half of the experimental schedule. Our mortality rate is difficult to compare with other Sinclair pigs series because most centers are purchasing animals at Sinclair facilities after diabetes induction, and mortality related to diabetes induction is not accounted for.

Diabetes induction by intravenous injection of 100–150 mg/kg of streptozotocin has been reported in minipigs and domestic pigs (7,28,29). We decided to inject streptozotocin intraarterially to increase its pancreatic concentration, as proposed by Tal et al (17) in a primate model. Instead of injecting into the celiac trunk after embolization of the gastric and hepatic arteries, we preferred injecting hyperselectively in the gastroduodenal and splenic arteries. This approach was successful in inducing diabetes with low rates of repeated streptozotocin injection and renal failure.

There are several limitations to this study. We selectively destroyed pancreatic beta cells with streptozotocin to decrease plasma insulin levels; this is not identical to early stages of human type 2 diabetes characterized by insulin resistance and concomitant hyperinsulinemia. This model would best represent the later stages of type 2 and type 1 diabetic patients with poor glycemic control and dyslipidemia (5). We used a suture with a rapid absorption profile that disappears completely by day 35 (27,28). This absorption time was perhaps too fast explaining why we observed less consistently advanced carotid plaques. More vulnerable lesions may have been observed with a suture with a slower absorption profile (polymer polyglycolic-lactic acid or standard Vicryl) and a longer follow-up (6–9mo). Finally, a lower mortality rate could have been observed by minimizing the number and the length of imaging procedures under general anesthesia.

In conclusion, the proposed model of accelerated atherosclerosis combining creation of carotid stenosis, diabetes, and hypercholesterolemia in pigs leads to advanced carotid, coronary, and femoral lesions within 5 months. The use of absorbable suture in the carotid artery is an innovation that may provide a more clinically relevant model for imaging and intervention studies.

REFERENCES

1. Casscells W, Naghavi M, Willerson JT. Vulnerable atherosclerotic plaque: a multifocal disease. Circulation 2003; 107:2072–2075.
2. Rosamond W., Flegal K., Furie K., et al. Heart disease and stroke statistics—2008 update: a report from the American Heart Association Statistics Committee and Stroke Statistics Subcommittee. Circulation 2008; 117:e25–e146.
3. Schwartz SM, Galis ZS, Rosenfeld ME, Falk E. Plaque rupture in humans and mice. Arterioscler Thromb Vasc Biol 2007; 27:705–713.
4. Boullion RD, Mokelke EA, Wamhoff BR, et al. Porcine model of diabetic dyslipidemia: insulin and feed algorithms for mimicking diabetes mellitus in humans. Comp Med 2003; 53:42–52.
5. Dixon JL, Stoops JD, Parker JL, Laughlin MH, Weisman GA, Sturek M. Dyslipidemia and vascular dysfunction in diabetic pigs fed an atherogenic diet. Arterioscler Thromb Vasc Biol 1999; 19:2981–2992.
6. Gerrity RG, Natarajan R, Nadler JL, Kimsey T. Diabetes-induced accelerated atherosclerosis in swine. Diabetes 2001; 50:1654–1665.
7. Larsen MO, Wilken M, Gotfredsen CF, Carr RD, Svendsen O, Rolin B. Mild streptozotocin diabetes in the Gottingen minipig: a novel model of moderate insulin deficiency and diabetes. Am J Physiol Endocrinol Metab 2002; 282:E1342–E1351.
8. Stary HC. Natural history and histological classification of atherosclerotic lesions: an update. Arterioscler Thromb Vasc Biol 2000; 20:1177–1178.
9. Virmani R, Kolodgie FD, Burke AP, Farb A, Schwartz SM. Lessons from sudden coronary death: a comprehensive morphological classification scheme for atherosclerotic lesions. Arterioscler Thromb Vasc Biol 2000; 20:1262–1275.
10. Mohler ER 3rd, Sarov-Blat L, Shi Y, et al. Site-specific atherogenic gene expression correlates with subsequent variable lesion development in coronary and peripheral vasculature. Arterioscler Thromb Vasc Biol 2008; 28:850–855.
11. Steele PM, Chesebro JH, Stanson AW, et al. Balloon angioplasty: natural history of the pathophysiological response to injury in a pig model. Circ Res 1985; 57:105–112.
12. Lam JY, Lacoste L, Bourassa MG. Cilazapril and early atherosclerotic changes after balloon injury of porcine carotid arteries. Circulation 1992; 85:1542–1547.
13. Narayanaswamy M, Wright KC, Kandarpa K. Animal models for atherosclerosis, restenosis, and endovascular graft research. J Vasc Interv Radiol 2000; 11:5–17.
14. Recchia D, Abendschein DR, Saffitz JE, Wickline SA. The biologic behavior of balloon hyperinflation-induced arterial lesions in hypercholesterolemic pigs depends on the presence of foam cells. Arterioscler Thromb Vasc Biol 1995; 15:924–929.
15. Ishii A, Vinuela F, Murayama Y, et al. Swine model of carotid artery atherosclerosis: experimental induction by surgical partial ligation and dietary hypercholesterolemia. AJNR Am J Neuroradiol 2006; 27: 1893–1899.
16. Shi ZS, Feng L, He X, et al. Vulnerable plaque in a swine model of carotid atherosclerosis. AJNR Am J Neuroradiol 2009; 30:469–472.
17. Tal MG, Hirshberg B, Neeman Z, et al. Induction of diabetes in nonhuman primates by means of temporary arterial embolization and selective arterial injection of streptozotocin. Radiology 2004; 230:163–168.
18. Grant EG, Benson CB, Moneta GL, et al. Carotid artery stenosis: gray-scale and Doppler US diagnosis—Society of Radiologists in Ultrasound Consensus Conference. Radiology 2003; 229:340–346.
19. Beneficial effect of carotid endarterectomy in symptomatic patients with high-grade carotid stenosis. North American Symptomatic Carotid Endarterectomy Trial Collaborators. N Engl J Med 1991; 325: 445–453.
20. American Diabetes Association. Diagnosis and classification of diabetes mellitus. Diabetes Care 2010; 33(Suppl 1):S62–S69.

21. Bellinger DA, Merricks EP, Nichols TC. Swine models of type 2 diabetes mellitus: insulin resistance, glucose tolerance, and cardiovascular complications. ILAR J 2006; 47:243–258.
22. Bonora E, Kiechl S, Willeit J, et al. Carotid atherosclerosis and coronary heart disease in the metabolic syndrome: prospective data from the Bruneck study. Diabetes Care 2003; 26:1251–1257.
23. van Kuijk JP, Flu WJ, Chonchol M, Bax JJ, Verhagen HJ, Poldermans D. Metabolic syndrome is an independent predictor of cardiovascular events in high-risk patients with occlusive and aneurysmatic peripheral arterial disease. Atherosclerosis 2010; 210:596–601.
24. Cunningham KS, Gotlieb AI. The role of shear stress in the pathogenesis of atherosclerosis. Lab Invest 2005; 85:9–23.
25. Schmitt C, Soulez G, Maurice RL, Giroux MF, Cloutier G. Noninvasive vascular elastography: toward a complementary characterization tool of atherosclerosis in carotid arteries. Ultrasound Med Biol 2007; 33: 1841–1858.
26. Granada JF, Kaluza GL, Wilensky RL, Biedermann BC, Schwartz RS, Falk E. Porcine models of coronary atherosclerosis and vulnerable plaque for imaging and interventional research. EuroIntervention 2009; 5: 140–148.
27. Swindle MM, Smith AC, Hepburn BJ. Swine as models in experimental surgery. J Invest Surg 1988; 1:65–79.
28. Grussner R, Nakhleh R, Grussner A, Tomadze G, Diem P, Sutherland D. Streptozotocin-induced diabetes mellitus in pigs. Horm Metab Res 1993; 25:199–203.
29. Wilson JD, Dhall DP, Simeonovic CJ, Lafferty KJ. Induction and management of diabetes mellitus in the pig. Aust J Exp Biol Med Sci 1986; 64:489–500.

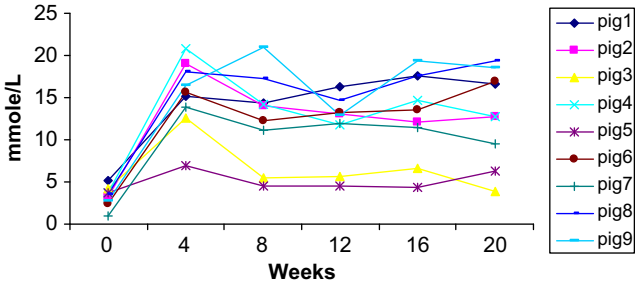

Figure E1. Evolution of blood glucose profile at baseline (T0) and during the 20-week follow-up period (T4, T8, T12, T16, T20).

Table E1. Distribution of Coronary and Femoral Artery Lesions According to American Heart Association Classification

Pig No.	RCA	LDA	Circumflex	Right Femoral	Left Femoral
1	V	III	III	NA	NA
2	II	II	II	NA	NA
3	II	II	0	0	0
4	VI	VI	VI	V	V
5	I	I	0	II	II
6	0	0	0	0	0
7	V	IV	III	I	I
8	I	IV	0	I	I
9	I	0	0	0	0

LDA = left descending coronary artery, NA = not available, RCA = right coronary artery.

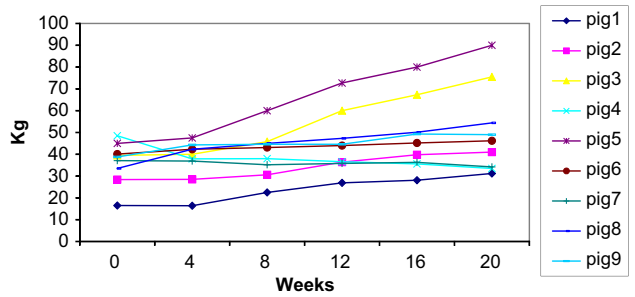

Figure E2. Evolution of weight curves at baseline (T0) and during the 20-week follow-up period (T4, T8, T12, T16, T20).

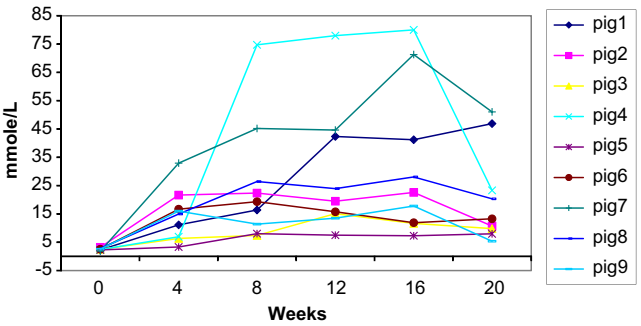

Figure E3. Evolution of total cholesterol at baseline (T0) and during the 20-week follow-up period (T4, T8, T12, T16, T20).

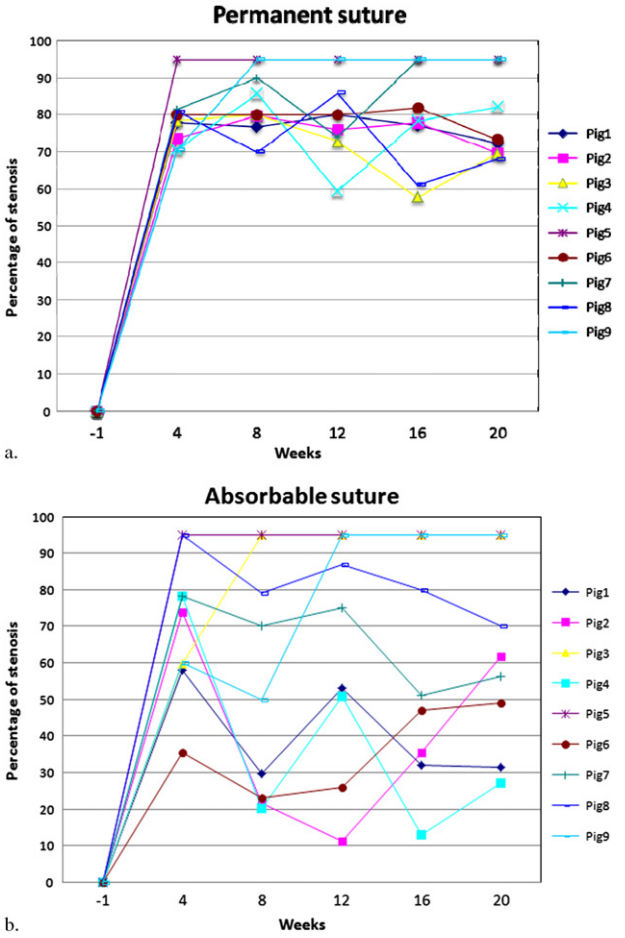

Figure E4. Evolution of carotid stenoses on Doppler US at baseline (T−1) and during the 20-week follow-up period (T4, T8, T12, T16, T20). Carotid suturing was performed at T0. **(a)** Carotid arteries sutured with permanent suture. **(b)** Carotid arteries sutured with absorbable suture.

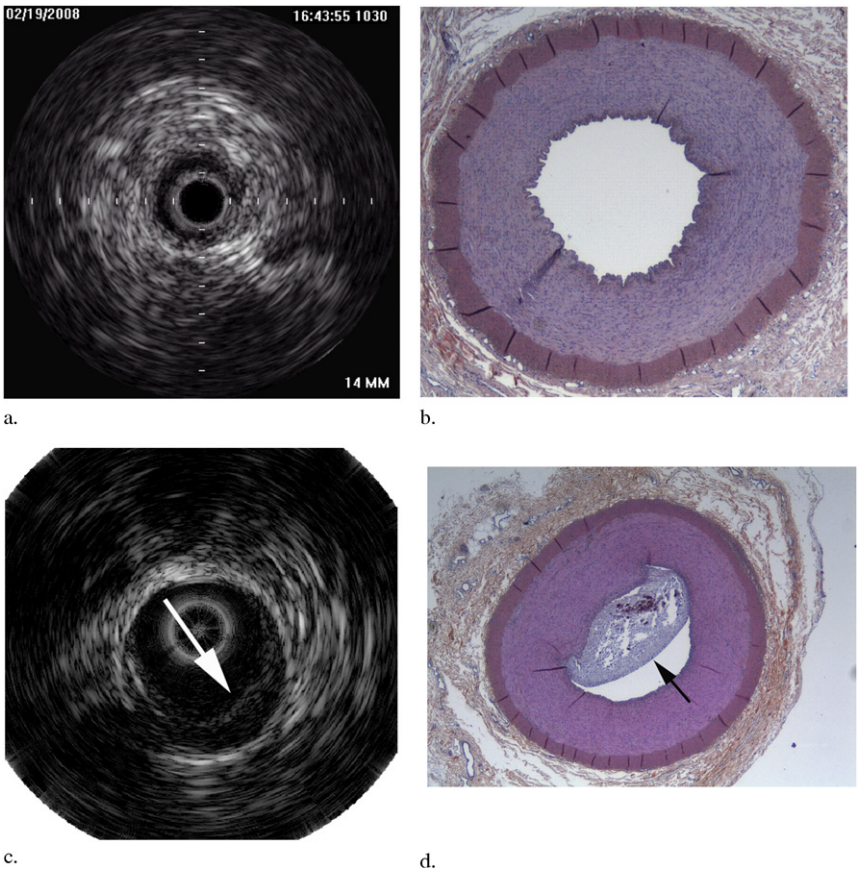

Figure E5. Vulnerable carotid plaque localized in the vicinity of a permanent suture (pig no. 4). Intravascular US **(a)** and histopathologic **(b)** examinations at the level of the suture show luminal narrowing and intimal hyperplasia. Intravascular US **(c)** and histopathologic **(d)** examinations acquired 5 mm cranially to the stricture show intimal hyperplasia, hypoechoic plaque with a lipid-rich necrotic core, and intraplaque hemorrhage (stage VI) (arrows).

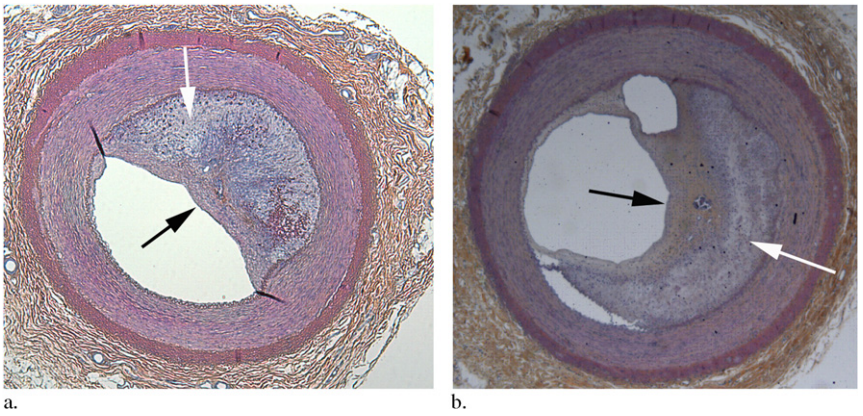

Figure E6. Development of bilateral near occlusion with advanced plaque formation (pig no. 9). Histopathologic examinations (**a** [right side] and **b** [left side]) show bilateral advanced atherosclerotic lesions with a lipid-rich necrotic core (white arrow) and fibrous cap (black arrow) (stage V).

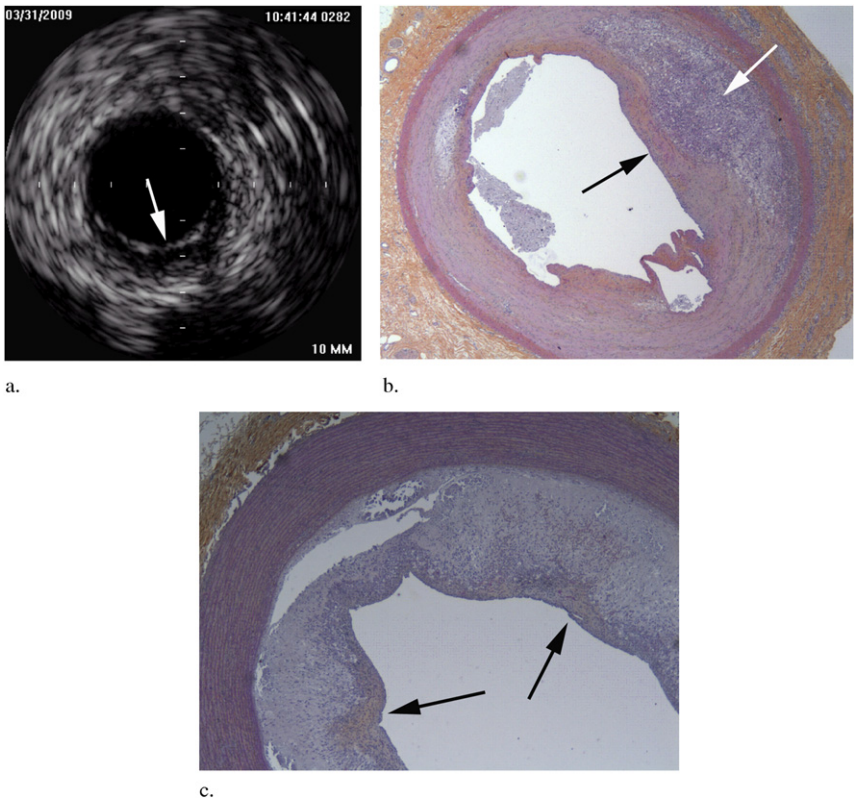

Figure E7. Development of an advanced atherosclerotic lesion after creation of carotid artery stenosis with an absorbable suture (pig no. 8). **(a)** Intravascular US shows a hypoechoic plaque lined by a hyperechoic intimal layer (arrow). **(b)** Histopathologic examination shows an advanced plaque with a lipid-rich necrotic core (white arrow) and a thick fibrous cap (black arrow) (stage V). **(c)** Another stage V plaque was also present proximal to the site of the arterial suture (arrows).

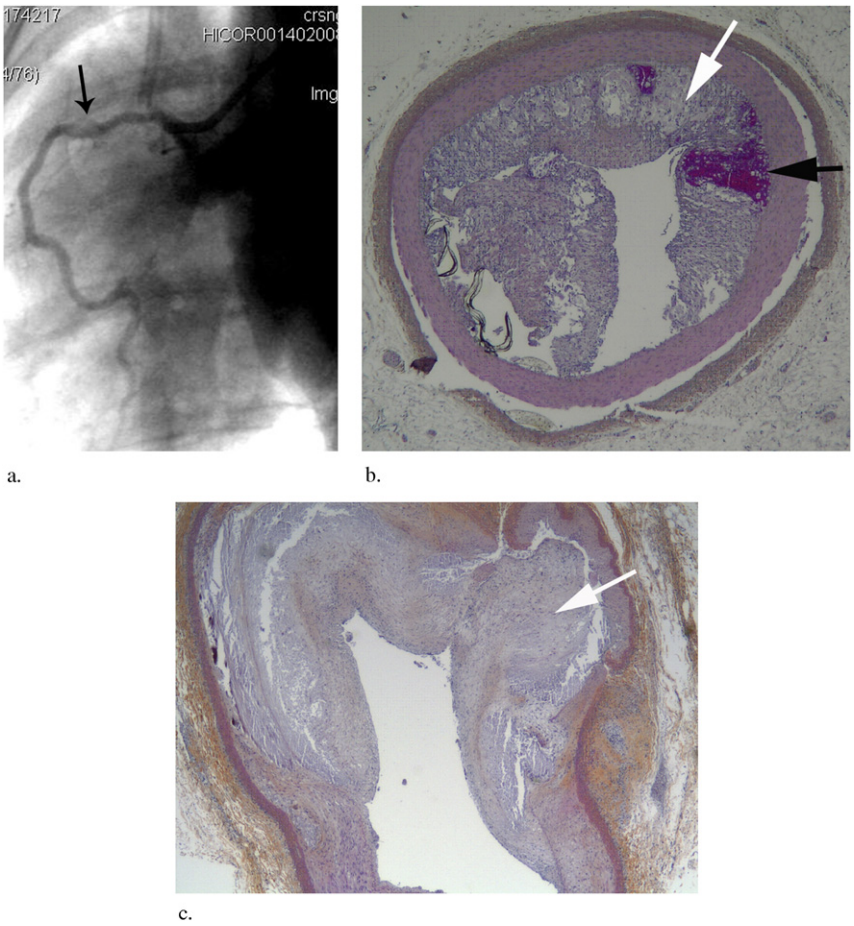

Figure E8. Development of advanced atherosclerotic lesions in coronary and femoral arteries (pig no. 4). **(a)** Right coronary angiography shows significant stenosis (arrow). **(b)** Histopathologic examination of the right coronary artery shows an advanced atherosclerotic lesion with a lipid-rich necrotic core (white arrow) and plaque hemorrhage (black arrow) (stage VI). **(c)** Histopathologic examination of the right femoral artery shows an advanced atherosclerotic lesion with a lipid-rich necrotic core (stage V) (white arrow).